Environmental heterogeneity patterns plant species richness and turnover in two hyperdiverse floras

Ruan van Mazijk, Michael D. Cramer & G. Anthony Verboom

Department of Biological Sciences, University of Cape Town, Rondebosch, South Africa

Corresponding author: RVM (ruanvmazijk@gmail.com, +27 21 650 3684)

ORCID nos.: RVM: 0000-0003-2659-6909, MDC: 0000-0003-0989-3266, GAV: 0000-0002-1363-9781

1 ## Abstract

2 **Aim:**

3 **Location:** The Greater Cape Floristic Region in southwest Africa (the Cape), and the Southwest Australia
4 Floristic Region (SWA)

5 **Taxon:** Vascular plants

6 **Methods:** Geospatially explicit floral and environmental data, non-parametric statistics, boosted regression
7 tree modelling

8 **Results:** The Cape is more environmentally heterogeneous and has higher levels of floristic turnover than
9 SWA. We find that environmental heterogeneity is the main predictor of species richness in the Cape, and
10 somewhat less so for SWA. Edaphic conditions are found to be of more biologically important in the Cape,
11 though this is contingent on the quality of the data modelled.

12 **Main conclusions:**

13 *Keywords:* biodiversity, environmental heterogeneity, fynbos, Greater Cape Floristic Region, kwongan,

macroecology, species richness, species turnover, vascular plants, Southwest Australia Floristic Region

1 Introduction

Biodiversity represents the variety of species and the ecological and evolutionary processes that bring about those species (**???**; Bøhn & Amundsen, 2004). Studying the distribution of biodiversity in space is a major avenue of biological research (**???**; Kreft & Jetz, 2007). Regional-scale geographic patterns in species richness have long been studied, particularly in biodiversity hotspots (**???**; Cook et al., 2015). The spatial distribution of species richness can be explained in terms of the physical environment. Properties of the environment have been suggested to influence species richness in three ways: (i) resources and energy, which can determine the number of species able to co-exist in an area (Gaston, 2000; Kreft & Jetz, 2007; Mouchet et al., 2015); (ii) stability through time, which enables species' persistence; and (iii) spatial heterogeneity, which can stimulate ecological speciation and possible barriers to gene flow and can facilitate greater levels of species' co-existence (Thuiller et al., 2006; Mouchet et al., 2015; Cramer & Verboom, 2016). The physical environment, then, can be used to explain species richness in both a local-deterministic and historical sense (Ricklefs, 1987).

The maintenance of species richness, particularly the coexistence of high numbers of species in biodiversity hotspots, is often regarded as "paradoxical" (Hart et al., 2017), and is a central problem in ecology (Ricklefs, 1987; Kreft & Jetz, 2007; Hart et al., 2017). Species richness is constrained by the ability of habitats to support a variety of species—its ecological carrying capacity (Mateo et al., 2017). This is exemplified in modelling approches, wherein species richness is a function of environmental predictors in a correlative framework ("macro-ecological models"; Mateo et al., 2017). Macroecological models of species richness implicitly

40 assume that communities are saturated, following species-area and species-energy relationships, and at

41 equilibrium with the environment (Mateo et al., 2017).

42 A solution to the "paradox" of species co-existence is environmental heterogeneity (EH): a more heterogeneous

43 environment gives rise to a larger environmental space, and can thus facilitate co-existence between more

44 species, generating more diverse species assemblages. Heterogeneity in the physical environment is known to

45 be positively associated with species richness (Rensburg et al., 2002; Hart et al., 2017), and has been

46 demonstrated to do so across many taxa—e.g. Canadian butterflies (**???**), European vertebrates (Mouchet et al.,

47 2015), South African birds (Rensburg et al., 2002), in communities along marine continental margins (Levin et

48 al., 2010), French scarab beetles (Lobo et al., 2004), and for global terrestrial plants (Kreft & Jetz, 2007). The

49 spatial scale of heterogeneity, or "grain" of the environment, is also important to consider (Hart et al., 2017), as

50 spatial scale in absolute environmental conditions has also been explored (**???**; Baudena et al., 2015; Mouchet

51 et al., 2015). Species co-existence and biodiversity maintenance is indeed suggested to be scale-dependent

52 (Hart et al., 2017).

53 EH is often under-represented in macro-ecological models of species richness, and has recently been found to

54 explain up to ca. 95% of biome level species richness across South Africa (Cramer & Verboom, 2016). Indeed,

55 models that include EH yield better estimates of the richness of the Cape flora (Thuiller et al., 2006; Cramer &

56 Verboom, 2016). Mediterranean-type terrestrial biodiversity hotspots, such as the Cape flora included in the

57 models by Cramer & Verboom (2016), present interesting study systems in which to investigate the relationship

58 between the environment and species richness. These systems exhibit far greater species richness than

59 predicted by their areas, productivities and latitudes (Cowling et al., 1996; Kreft & Jetz, 2007). There are five

60 Mediterranean biodiversity hotspots on Earth: the California Floristic Province, the Mediterranean Basin, the

61 Chilean Winter Rainfall-Valdivian Forests, the Greater Cape Floristic Region, and the Southwest Australia

62 Floristic Region (Cowling et al., 1996; Hopper & Gioia, 2004; Cook et al., 2015). These ecosystems have

63 regular fire-cycles (Cowling et al., 1996), climatic buffering, and long term stability (Kreft & Jetz, 2007),

64 shrubby, sclerophyllous flora (Hopper & Gioia, 2004). Together, they account for ca. 20% of global vascular

65 plant species, yet only ca. 5% of global land surface areas (Cowling et al., 1996). Various hypotheses have

66 been proposed to explain the high levels of plant species richness in these regions (Cook et al., 2015). The

67 species accumulation hypothesis states that the stability of these regions has allowed many species to accrue.

68 The species co-existence hypothesis states that these hotspots may facilitate greater degrees of species

69 co-existence in smaller spatial areas, due to fine-scale heterogeneity in their environments. Indeed, EH has

70 evolutionary implications too, stimulating ecological speciation across sharp environmental gradients.

71 Both the Southwest Australia Floristic Region (SWA) and the Greater Cape Floristic Region (Cape) are

72 Mediterranean-type biodiversity hotspots, particularly in terms of plant species. Where the Cape (with an area

73 of ca. 189,000 km^2) is known to contain about 11,400 plant species (about 0.060 species per km^2), SWA (area

74 of ca. 270,000 km^2) has about 3,700 species (0.014 species per km^2) (**???**). So, the Cape has ca. 4.3 times as

75 many species per km^2 as SWA. The Cape and SWA are appropriately often compared, due to the similarities

76 between their environments (e.g. oligotrophic soils, an oceanically buffered moderate climate) and their plants'

77 ecologies (Hopper & Gioia, 2004). These two regions present unique flora out of the five Mediterranean

78 systems, with high levels of endemism (Cowling et al., 1996), and many obligate fire-adapted species (Cowling

79 et al., 1996). Similarities withstanding, SWA is topographically and edaphically distinct from the Cape. The

80 former is topographically rather uniform (i.e. flat)—uniquely so among the world's five Mediterranean-climate

81 regions (Hopper & Gioia, 2004)). SWA possesses a mesoscale chronosequence dune system (Laliberte et al.,

82 2014; Cook et al., 2015), while the Cape is mountainous, topographically heterogeneous, and therefore

83 associated with a large degree of spatial climatic variability, with a fine-scale mosaic of geologies and soils

84 (Cowling et al., 1996; Cramer et al., 2014; Verboom et al., 2017).

85 Both regions have sources of edaphic heterogeneity, but at different scales. This edaphic variability may aid in

86 explaining the species richness in these regions (Beard et al., 2000; Verboom et al., 2017). EH of many forms

87 will likely be important in macro-ecological models in both regions, as both regions have been relatively

88 environmentally stable over evolutionary time-scales (Wardell-Johnson & Horwitz, 1996; Hopper & Gioia,

89 2004; Lambers et al., 2010; Cramer et al., 2014; Laliberte et al., 2014; Cook et al., 2015). For the Cape, high

90 levels of species richness are thought to result from long term climatic stability, and fine grain variation in

91 geology and soils (Cramer et al., 2014). The question thus arises whether heterogeneity is a significant

92 contributor to SWA species richness. In the absence of topographic variability in SWA, it is proposed that the

93 heterogeneity of that region is due to the juxtaposition of soil types (Laliberte et al., 2014; Cook et al., 2015),

94 creating extreme edaphic variation.

95 Our hypotheses concern the Cape and SWA's environments and floras. Our main hypothesis is that the Cape

96 possesses greater abiotic heterogeneity, and at finer grain, compared to SWA, such as to explain the Cape's

97 greater species richness per unit area, and proposed greater levels of species turnover between areas. We also

98 conjecture that the heterogeneity that predicts species richness in SWA will be more pronounced in terms of

99 edaphic variables. Here we attempt to assess five key predictions of this hypothesis, additionally investigating

100 a seventh prediction to test the conjectured role of edaphic heterogeneity in SWA. Dealing with the two

101 regions' environments, we assess (i) whether the Cape environment is more heterogeneous than that of SWA

4

and (ii) whether the Cape environment has more pronounced heterogeneity at finer scales than that of SWA. Dealing with the distribution of species in the two regions, we assess (iii) whether the Cape exhibits greater levels of species turnover between areas. Relating each regions' environment and flora, we finally assess (iv) whether species richness and species turnover are adequately predicted by EH in both regions and whether (v) species richness and species turnover are better predicted by different forms of EH in either region (e.g. the importance of edaphic heterogeneity in SWA).

2   Materials and methods

2.1   Overview

Our analyses defined boundaries for each region, those regions' environmental data and geospatially-explicit vascular plant occurrence records, all based on publicly available data. The environmental variables chosen (Table 1) for this study were intended to cover a reasonable spread of climatic, edaphic, and ecologically relevant environmental axes, and are not intended to be exhaustive. We selected variables describing topography (elevation), productivity (NDVI), soil status and climate and climatic seasonality.

We carried out this investigation at four principal spatial scales: 0.05º x 0.05º squares (the finest common resolution among the environmental data sources used), quarter degree squares (QDS) (Larsen et al., 2009), half degree squares (HDS) (Larsen et al., 2009) and three-quarter degree squares (3QDS). For the Cape, most plant occurrence records are only accurate to QDS level. Thus, analyses involving species occurence data were necessary limited to scales including and above QDS.

Analyses were performed in R v3.4.0–3.5.1 (R Core Team, 2018). Version-numbers of specific R packages used are presented in the bibliography.

2.2   Environmental data sources

The GCFR was treated as the areas occupied by the Succulent Karoo and Fynbos biomes in the current delineation of South Africa's biome boundaries (Mucina & Rutherford, 2006). The SWAFR was treated as the areas occupied by the Southwest Australia savanna, Swan Coastal Plain Scrub and Woodlands, Jarrah-Karri forest and shrublands, Southwest Australia woodlands, Esperance mallee, and Coolgardie woodlands in the

127 World Wildlife Fund Terrestrial Ecoregions dataset (Olson et al., 2001) in order to closely match the currently

128 delineated SWAFR (Gioia & Hopper, 2017, Hopper & Gioia (2004)). For the sake of readability, we shall refer

129 to the GCFR and SWAFR simply as the Cape and SWA from hereon.

130 Geospatially-explicit raster layers were acquired for a selection of environmental variables (Table 1), for the

131 regions of interest. Raster data were re-projected to a common coordinate reference: WGS84 (NIMA, 2000),

132 using the "rgdal" (**???**) package in R (R Core Team, 2018). All data were re-sampled to 0.05º resolution using

133 the "resample" function in the R package "raster" (**???**), with the "bilinear" method.

134 An emphasis was made on using satellite-derived environmental data in this work, in order to minimise

135 differences in data quality and methodologies between the Cape and SWA. Additionally, satellite-derived data

136 have been shown to benefit regional-scale species distribution models (Deblauwe et al., 2016), thus motivating

137 their use in this regional-scale study. The environmental data used in this study were derived from NASA's

138 SRTM digital elevation model (Farr et al., 2007), NASA's MODIS/Terra spectroradiometric data for land

139 surface temperature and NDVI, the Climate Hazards Group's CHIRPS rainfall dataset (Funk et al., 2015), and

140 the International Soil Reference and Information Centre's SoilGrids250m edaphic dataset (Hengl et al., 2017)

141 (Table 1). SRTM and MODIS are entirely derived from satellite measurements, whereas CHIRPS is

142 interpolated from weather station data with satellite-derived radiometric measurements. SoilGrids250m is a

143 machine-learning derived product, based on soil measurements as a function of many covariates, including

144 MODIS and STRM sources (see Hengl et al., 2017), using random-forests and other classification-tree-based

145 methods, including gradient-boosting. For the soil data considered here (Table 1), we used depth-interval

146 weighted average values as the value for a particular soil variable in a given place.

147 Climatic and spectral data arise from satellites monitoring properties of the Earth's surface through time. We

148 therefore use the mean annual values for rainfall, surface temperature, and NDVI in each pixel in our analyses.

149 Pronounced seasonality of rainfall is a known feature of mediterranean systems (**???**). We describe this

150 seasonality by computing computing the precipitation in the driest quarter (PDQ), using methods based on the

151 "biovars" function in the R package "dismo".

2.3   Plant occurrence data

153 Geospatially-explicit records of vascular plant occurrences were downloaded from the Global Biodiversity

154 Information Facility (GBIF, Table 1). Queries were made for tracheophyte records from within the borders of

155 the Cape and SWA as treated here (GBIF, 24 July 2017, GBIF (24 July 2017)). Only records with defined

156 species and intra-specific ranks were kept. Intra-specific occurrences were treated as simply being

157 representative of their species. This resulted in FIXME unique species names in the Cape, and FIXME in SWA.

158 We cleaned these data using the R package "taxise" (**???**, (**???**)) to check that these species names had

159 accepted-status among taxonomic databases. We queried two major taxonomic databases: the Global Name

160 Resolver (GNR), and the Taxonomic Name Resolution Service (TNRS). Should either one of these services

161 return at least one match for a given name, then that name was accepted. Those names for which no full

162 binomial matches were found in either database were excluded from the final list of species. The number of

163 species names excluded totalled at FIXME and FIXME for the Cape and SWA respectively. Especially for

164 SWA, these numbers may be deemed appreciably high. But, the occurrence records that would be dropped, as a

165 consequence of these names' removals, appeared randomly distributed in geographic space in both regions. As

166 such, any effect of the loss of these records in this analysis is likely uniform within the two regions.

167 After the unaccepted names were removed, it was important to ensure that a species was not listed under

168 multiple synonyms. Such cases would skew estimates of species richness and turnover in this study. In light of

169 this, the remaining names were queried in the Tropicos and Integrated Taxonomic Information System (ITIS)

170 databases for their known synonyms, again using "taxize". These were collated to produce a nomenclatural

171 "thesaurus" for the Cape and SWA species. This consisted of a list of the accepted species names in a region,

172 each associated with a list of known synonyms. We amended species' names in the GBIF occurrence data, in

173 order ensure species were listed under only one of these synonyms, replacing all appearances of a species'

174 synonyms with the first synonym used in the list.

175 Lastly, We removed any species from both regions that are invasive aliens or non-indigenous. Alien species

176 lists for plants in South Africa and Australia were acquired from the IUCN's Global Invasive Species Database

177 (http://www.iucngisd.org/gisd/).

178 The final total plant species richness in each region was FIXME and FIXME for the Cape and SWA

179 respectively. These final collections of species occurrence records were converted to raster-layers, wherein

180 pixel-values represented the species richness of vascular plants within that pixel. These rasters were produced

181 at QDS, HDS, and 3QDS resolutions.

2.4 Analyses

2.4.1 Quantifying environmental heterogeneity

In order to assess predictions (i) and (ii), we needed to describe the EH in both regions. Using the R package "raster" (**???**), we used a modified version of the "roughness" index in the "terrain" function. For a three by three neighbourhood $\mathbf{N}$ of cells, our index of roughness R is the average square-root of the squared difference between each of the n neighbour cells' values x_i and the central focal cell's value x_{focal}:

$$R(\mathbf{N}) = \frac{1}{n} \sqrt{\sum_{i=1}^{n} \left(x_{\text{focal}} - x_i \right)^2} \tag{1}$$

This value, notionally equivalent to the standard deviation of values relative to the focal value, is ascribed to the focal cell. Note, in order to use as much data from within regions' borders as possible, roughness was computed if a focal cell had at least one neighbour cell. Using this index, we produced raster layers of each of our nine environmental variable's heterogeneity. We compared the distributions of "roughness" values in each variable in each region with non-parametric Mann-Whitney U-tests, as almost all variables were highly non-normal, and could not be normalised by log-transformations. We also compare the effect size of the Cape vs SWA using the "common language effect size" ($CLES$), using the R package "canprot". The $CLES$ is the proportion of all pairwise comparisons between two sample groups' observations where one group's value is greater than the other's. We calculated the $CLES$ as the proportion of pairs where Cape roughness values were greater than that of SWA. This allowed us to assess prediction (i). To compare the spatial scales of heterogeneity (prediction (ii)) between each region, we repeated this analysis at all four spatial scales. This entailed recalculating the roughness layer for each variable after the original layer (0.05 degrees resolution) had been rescaled to each of the coarser resolutions.

2.4.2 Quantifying species turnover

Regarding prediction (iii), we wished to compare the general degree of species turnover in each region. To compare the extent of species turnover between the Cape and SWA, we determined two metrics of species turnover. The first, computes the mean species turnover as Jaccard distances (**???**) between each pair of QDS within each HDS ($\overline{J}_{\text{QDS}}$, based on HDS with $2 \leq n \leq 4$ QDS) in both regions. The second is defined in terms of Whittaker's additive definition of β-diversity (**???**), as follows:

$$\gamma = \alpha + \beta \tag{2}$$

207 Here, we treat species richness at the HDS-scale (S_{HDS}) as γ-diversity and at the QDS-scale ($\overline{S}_{\mathrm{QDS}}$) as

208 α-diversity. Intuitively, the species richness of an area is the result of some combination of the richness of sites

209 within that area and the difference in species complements between those sites. Thus, we partition γ-diversity

210 as in Equation (2), such that β-diversity is the difference between γ- and α-diversity. We compare the

211 distributions of $\overline{J}_{\mathrm{QDS}}$ and T_{HDS} using non-parametric Mann-Whitney U-tests, in order to guard against

212 non-normality.

213 2.4.3 Predicting richness and turnover with environmental heterogeneity

214 Regarding prediction (iii), we wished to compare the general degree of species turnover in each region. For (iv)

215 and (v) we modelled species richness (S) and turnover as a function of various combinations of environmental

216 and environmental heterogeneity variables in both regions using boosted regression-tree (BRT) modelling

217 techniques. This allowed us to explore which axes of environmental heterogeneity are most influential on

218 vascular plant species richness and turnover, and the differences in the importance of such axes between the

219 Cape and SWA.

220 BRTs are a flexible machine learning-based model of response variables and do so without involving normal

221 null-hypothesis significance testing (Elith et al., 2008), and have been employed previously to model species

222 richness (Thuiller et al., 2006; see Mouchet et al., 2015; Cramer & Verboom, 2016) as macro-ecological

223 models. BRTs are developed through the iterative generation of non-linear regression trees. BRTs are an

224 ensemble-approach, in which a prediction $\widehat{y_i}$ is based on the weighted sum of the predictions of progressively

225 "less important" regression trees (t_k), as opposed to the predictions of one tree (Elith et al., 2008). For $k \to nt$

226 number of trees, where each tree is itself a function of the matrix $\mathbf{X}$ of j predictor variables ($t_k = f(x_{ij})$), a

227 BRT-model can be represented as follows:

$$\widehat{y_i} = \sum_{k=1}^{nt} w_k t_k \tag{3}$$

228 BRTs have two major meta-parameters over which users have control (**???**): the learning rate (lr, the rate at

229 which iterative trees reduce predictive deviance during model-training, controlling the contribution of each tree

230 to the final model) and tree complexity (tc, the number of nodes on a given regression-tree, i.e. the maximum

231 interaction depth the model is permitted to fit).

232 BRTs were implemented here to predict both vascular plant species richness and turnover in each HDS, as a

233 function of environmental variables and environmental roughness values in those cells, as Gaussian responses,

234 thus resulting in two BRT-models for each region. We treated richness as S_{HDS} and turnover as $\overline{J}_{QDS}$. The

235 natural logarithm of species richness was used, in order to satisfy the assumptions of a Gaussian response.

236 Note, this is not strictly because BRTs have any parametric assumptions concerning the distribution of the

237 response variable, but rather to aid in applying the Gaussian-family of BRT algorithms to the richness data

238 available. Additionally, BRTs were implemented to predict vascular plant species richness at the QDS-scale

239 (S_{QDS}), thus resulting in a total of six BRT-models presented here.

240 As recommended by Elith et al. (2008), BRT models were trained on a set of non-collinear predictor variables

241 using "gbm.step" in "dismo" (**???**) and "gbm" (**???**). Collinear predictor variables can skew the interpretation

242 of results, as the relatively influence of mutually collinear variables is reduced. Collinearity among the nine

243 environmental predictor variables and their respective nine roughness-equivalents was assessed using

244 "removeCollinearity" in the R package "virtualspecies" (**???**) separately for each region, such that variables

245 were no more than 80% collinear (Pearson's $r \geq 0.80$). When faced with a cluster of collinear variables, one

246 variable was chosen manually therefrom. Where possible, the roughness-equivalent of an environmental

247 variable was included if its absolute-equivalent could also be included. When interpreting the results of BRTs,

248 it is important to consider the effects of the variables included as representative of the effect of the excluded

249 variables with which it was found to be collinear.

250 In order to select ideal lr and tc all models (described below) were trained on the final non-collinear predictor

251 sets iteratively for 25 combinations of a range of tc values (1 to 5) and a range of lr values (0.01, 0.005, 0.001,

252 5×10^{-4}, 1×10^{-4}). The function "gbm.step" optimises the number of trees (nt) using cross-validation during

253 model training (Elith et al., 2008) by halting iteration when predictions begin to overfit. For all models, we

254 used 10 cross-validation folds (i.e. use 10 different randomly selected training data sets), a tolerance-threshold

255 of 0.001, a bagging-fraction of 0.75 (proportion of training data randomly chosen to generate each tree), and

256 trained models starting with 50 trees, with each iterative step adding 50 trees at a time, up to a maximum of

257 10,000 trees. Following this iterative parameter optimisation, Gaussian BRT models were constructed with

258 $tc = 3$ and $lr = 0.001$, along with the other settings described.

259 The optimum configuration of lr and tc for the final model is a trade-off between model fit (e.g. pseudo-R^2;

260 Equation (4)) and complexity (nt). A tc of 5 was chosen for the final model. This follows the

261 recommendations of Elith et al. (2008), where lr and tc are advised to be adjusted inversely. This was chosen

262 in order to account for the complex interactions determining species richness. To avoid overfitting, an

263 intermediate lr of 0.001 was chosen.

264 2.4.4 Assessing BRT-predictions' fit

265 BRT-model performance can be described by measuring the variance in a dataset a BRT-model has explained,

266 quantified here by R^2_{pseudo}, which is the proportion of null deviance D_{null} explained by some model i.

267 Formally, it is defined as follows:

$$R^2_{\text{pseudo}} = 1 - \frac{D_i}{D_{\text{null}}} \tag{4}$$

268 The derivation of this metric is not easy to interpret, as it is not immediately clear what model deviance is.

269 Alternatively, comparing expected (i.e. model-predicted) and observed data has more heuristic appeal. We

270 employed this metric of BRT-model performance too. We regressed expected against observed richness and

271 turnover, and calculated the R^2-value for those regressions (hereafter $R^2_{\text{E-O}}$).

272 The BRT-model fitting algorithm contains intrinsic stochasticity, due to the random partitions made in a dataset

273 during cross-validation. Though this randomness is usually negligible (e.g. variables' contributions vary from

274 run-to-run by a few decimal places), we reran each of the six BRT-models (see above) 1000 times in order to

275 account for this stochasticity. Where indicated, we either present the averages of these replicate-models' results

276 or the results of a representative model from each set of replicates.

277 In order to assess the reliability of the conclusions drawn from these models, we randomly permuted the

278 response data (S_{QDS}, S_{HDS} and $\overline{J}_{\text{QDS}}$) with respect to the environmental and heterogeneity data, and reran all

279 six BRT-models 999 times (with the final non-collinear predictor sets and preconfigurations above). This also

280 allows us to remove any effect of spatial autocorrelation in generating the observed correlations between

281 patterns of species occurrence and environment (**???**), and to allow us to assess the significance of our results

282 relative to a random null. Notably, as the predictor variables themselves are likely spatially autocorrelated,

283 correlation structure in model residuals is accounted for by the correlation structure in the environmental data.

284 Nonetheless, we wished to demonstrate our results more robustly and thus carried out these permutation tests.

285 For all six models, the majority of the 999 permuted models failed to find associations between the response

286 and predictor variables. The results of those that succeeded to fit a model to completion (usually ca. 200 out of

287 999) are presented. The replicate and permuted BRT-models were compared using various measures of model

288 performance (above; nt, R^2_{pseudo} (Equation (4)), $R^2_{\text{E}-\text{O}}$) and the ranks of these values for each replicate

289 BRT-model relative to the 999 permuted models for that region/scope.

3 Results

3.1 Describing environmental heterogeneity across scales

292 Across all variables considered, the Cape is more environmentally heterogeneous in the majority of pairwise

293 comparisons of grid-cells ($CLES > 0.50$, Mann-Whitney U-test: $P < 0.05$, Figure 1). The degree to which

294 the Cape is more heterogeneous varies between environmental variables. These effects also vary somewhat

295 across spatial scales. In some variables, the differentiation between Cape and SWA heterogeneity lessens at

296 coarser scales (Figure 1b). Indeed, when comparing the overall ranking and medians of Cape vs SWA

297 roughness values for each variable, we only find non-significant differences at the 3QDS scale (Mann-Whitney

298 U tests, $P > 0.05$, Figure 1b).

299 Most obviously, and as expected, topographic heterogeneity is generally greater in the Cape than in SWA

300 (Figure 1). Though SWA has a slightly wider distribution of elevational roughness values at coarse scales

301 compared to fine scales than the Cape, the relative difference in heterogeneity between the two regions seems

302 invariant with spatial scale ($CLES \approx 0.95$, Figure 1b). This concurs with our expectations, as the Cape is

303 mountainous and known to have steep elevational gradients (**???**), while SWA is much more topographically

304 uniform. Elevational roughness differs between the two regions in the manner we expected, giving us more

305 confidence in the environmental reality of our other results here.

306 Climatic heterogeneity is less differentiated between the Cape and SWA than with topographic heterogeneity

307 (Figure 1a), though the Cape is indeed more climatically heterogeneous (Figure **??**b). Notably, the difference

308 between roughness in mean annual rainfall (R MAP) and land surface temperature (R Surface T) in the Cape

309 and SWA is less pronounced when considered at coarse spatial scales (Figure **??**b). At all spatial scales

310 considered, roughness in rainfall seasonality (R PDQ), however, is equally more heterogeneous in the Cape

311 than SWA. Biological productivity, as measured by NDVI, is fairly similarly heterogeneous in the Cape and

312 SWA ($CLES < 0.60$, Figure 1). Concerning edaphic variables, the Cape and SWA are similarly

12

313 heterogeneous at coarser scales, particularly in terms of CEC and Soil C ($CLES \approx 0.50$, Figure 1b).

3.2 Comparing species turnover in the two regions

315 Following calculations of $\overline{J}_{\mathrm{QDS}}$ and T_{HDS} for each HDS-cell in each region, we also used non-parametric

316 Mann-Whitney U-tests to compare the distributions of values in the Cape and SWA. The Cape possesses

317 generally greater floristic turnover than SWA, for both measures of turnover defined here ($P < 0.0001$, Figure

318 2a,b). $\overline{J}_{\mathrm{QDS}}$ measures the average pairwise Jaccard distance between QDS-cells in each HDS-cell. T_{HDS},

319 however, represents the inferred β component of γ-diversity. As γ-diversity ($= S_{HDS}$) in the Cape has a

320 greater β-diversity component ($= T_{HDS}$) than SWA, the complement is necessarily true: γ-diversity in the

321 Cape has a lesser α-diversity component ($= \overline{S}_{\mathrm{QDS}}$) than SWA.

3.3 Predicting richness and turnover with environmental heterogeneity

323 We found vascular plant species richness and turnover both to be predicted primarily by environmental

324 heterogeneity in the Cape (Figure 3a–c) and at least in-part by environmental heterogeneity in SWA (Figure

325 3d–f). Our six BRT-models performed adequately, and detected relationships between patterns of species

326 occurrence and the environment that do not occur in the permuted datasets (Figures 4 and 3, Table 2).

327 BRT-models of species richness at the QDS-scale in each region generally performed best, as these models had

328 fit greater number of trees (nt, Figure 4a), and possess higher R^2-values (Figure 4b,c). SWA models of species

329 richness and turnover at the HDS-scale out-performed Cape models. At the QDS-scale, the Cape and SWA

330 models performed equally well (Figure 4, Table 3).

331 Across our BRT-models of species richness and turnover, the importance of different environmental variables

332 in predictions differed substantially between the Cape and SWA. Additonally, the relative importance of

333 absolute and heterogeneity variables also differs between the Cape and SWA (Figure 3). Most obviously,

334 species richness and turnover in the Cape are predicted mostly by environmental heterogeneity, which is not the

335 case in SWA (Figure 3). Species richness and turnover in the Cape are predicted by a broad suite of

336 environmental variables, with no individual variable contributing more than ca. 20% to any model prediction

337 (Figure 3a–c). The SWA models' predictions, however, are largely determined by MAP (Figure 3d–f).

338 Species richness at QDS-scales ($= \overline{S}_{\mathrm{QDS}}$), and to a lesser extent at HDS-scales ($= S_{\mathrm{HDS}}$), in the Cape is

13

339 predicted largely edaphic conditions (Figure 3a,b). Species richness in SWA, at both scales, is mostly predicted

340 by MAP and other climatic variables (Figure 3d,e). Interestingly, topograhphic heterogeneity did not feature as

341 highly in contributing to Cape predictions as we expected (Figure 3a–c).

342 It is important to consider variables not included formally in these BRT-models that were found to be collinear

343 with some of the variables included (see SI). Here, we interpret the effects of variables excluded from the

344 analyses as well as those included, as the forms and importances of these relationships are likely similar. In the

345 Cape (concerning clusters of collinear variables relevant to relevant to those retained during BRT-model

346 fitting), MAP was included in the BRT-analyses as representative of a cluster of collinear variables consisting

347 of itself, NDVI, surface T and soil C at the. Roughness in soil clay content represented itself, roughness in soil

348 pH and roughness in NDVI. In SWA, MAP was select as representative of itself, NDVI and soil C.

349 **In the equations below, collinear groups of variables are listed as predictors enclosed within braces.**

350 **Cape:**

$$\overline{S}_{\text{QDS}} \sim pH + RSurfT + \begin{Bmatrix} MAP \\ NDVI \\ SurfT \\ SoilC \end{Bmatrix} + \begin{Bmatrix} RClay \\ RpH \end{Bmatrix} + RElev$$

$$S_{\text{HDS}} \sim RSurfT + RElev + RCEC + \begin{Bmatrix} RMAP \\ RPDQ \\ RNDVI \end{Bmatrix} + \begin{Bmatrix} MAP \\ NDVI \\ SurfT \\ SoilC \end{Bmatrix}$$

$$T_{\text{HDS}} \sim RElev + RSurfT + \begin{Bmatrix} RMAP \\ RPDQ \\ RNDVI \end{Bmatrix} + Elev + RCEC$$

351 **SWA:**

$$\overline{S}_{\text{QDS}} \sim \begin{Bmatrix} MAP \\ NDVI \\ SoilC \end{Bmatrix} + PDQ + RMAP$$

$$S_{\text{HDS}} \sim \begin{Bmatrix} MAP \\ NDVI \\ SoilC \end{Bmatrix} + CEC + RElev$$

$$T_{\text{HDS}} \sim \begin{Bmatrix} MAP \\ NDVI \\ SoilC \end{Bmatrix} + RElev + CEC$$

352 Our BRT-models of species richness in both regions rank environmental variables somewhat differently at

353 QDS- and HDS-scales (Figure 3a,b,d,e). These differences in rankings are similar to those between two

354 unrelated lists ($P_{1-2} > 0.05$, Figure 5). This suggests some scale-dependence of different environmental

355 variables' associations with species richness.

356 It is noteworthy that BRT-models of species turnover ($= \overline{J}_{\text{QDS}}$, at HDS-scales) (Figure 3c,f) rank variables

357 similarly to models of richness at HDS-scales ($P_{2-3} \leq 0.005$, Figure 5). This is likely due to the fact that

358 proportional floristic turnover covaries with species richness. As such, though the signs of relationships

359 determining turnover may differ from those determining richness, the importances of different variables would

360 be similar.

361 In addition to different variables being more strongly associated with species richness and turnover in the Cape

362 compared to SWA (Figure 3), the forms of those relationships vary (Figure 6). We found MAP, and roughness

363 therein, to relate positively with species richness in both regions at both scales (Figure 6a,b,d,e). As MAP is

364 collinear with NDVI and soil C in both regions (and surface T in the Cape), this can be interpreted as the signal

365 of a biological productivity and resource availability associating with high levels of species richness.

366 The positive association of heterogeneity variables in the Cape as opposed to SWA (Figure 6a,b vs d,e) concurs

367 with their greater importance in BRT-model predictions (Figure 3).

368 The fact that species turnover ($T_{HDS} = \overline{J}_{QDS}$) in the Cape and SWA is largely predicted by the same

369 variables as species richness, but with opposite signs to its relationships (Figure 6c,f), is indicative of the

370 richness-dependence of the measure of floristic turnover used here (Jaccard distances) to quantify turnover at

371   the HDS-scale.

4   Discussion

373   I have provided support for the hypothesis that the difference in plant species richness between the GCFR and

374   SWAFR is accounted for by the fact that the GCFR is more abiotically heterogeneous than the SWAFR. As

375   expected, the GCFR is shown to possess (i) a quantifiably more heterogeneous environment, and (ii) is

376   heterogeneous at a finer spatial scale than the SWAFR. I have shown that vascular plant species richness (iii)

377   can be explained in terms of environmental conditions, including environmental heterogeneity, in both the

378   GCFR and SWAFR. Also, I have shown that (iv) the set of environmental axes that explain plant species

379   richness, both absolute and as heterogeneity, differs between the GCFR and SWAFR. These findings contribute

380   towards an understanding of the ecological conditions that facilitate species coexistence (and likely stimulate

381   ecological speciation) in these two regions.

382   These two regions present differentiable environmental spaces, each with heterogeneity varying across spatial

383   scales. The clear separation of the regions' topographic features is as expected (Figures **??**A, **??**). Indeed,

384   topography seems to be the most striking distinction between the regions. The Cape region has been found

385   previously to have the second highest median topographic heterogeneity of the five Mediterranean-climate

386   regions (Bradshaw & Cowling, 2014). The GCFR has a much wider range of scales exhibited in the

387   heterogeneity across its environmental axes. Notably, each region has finer scale heterogeneity in some

388   variables, and coarser scale in others—neither region is necessarily more fine or coarse than the other, as it

389   depends on the variable concerned. BRT-models of species richness in both regions reveal species richness to

390   depend on those environmental axes that differentiate the two regions (Figures **??**), **??**). The importance of

391   variables is also shown to vary with spatial scale (Figure **??**), as previously suggested may be the case when

392   modelling geographic patterns of biodiversity (Baudena et al., 2015). Indeed, as Cowling et al. (1996)

393   describes differing patterns of species richness across spatial scales, so do the predictors of those patterns vary

394   with scale (Hart et al., 2017).

395   The fact that a combination of absolute and roughness variables is also as predicted by the hypothesis in this

396   study. In the models developed by Cramer & Verboom (2016) for South Africa, roughness in topography was

397   largely superseded as an important predictor of species richness by other roughness variables. My models,

398   however, did not show this. Similar to the study by Rensburg et al. (2002), my models revealed roughness in

16

topography and other variables to be important. Although, Rensburg et al. (2002) considered differences within pixels, as opposed to this study, which considered differences between pixels. My models, those of Cramer & Verboom (2016), and those of Rensburg et al. (2002), do not all concur as to the role of roughness in elevation vs. more biologically meaningful variables in explaining species richness. The source of these discrepancies is unclear, though no doubt complex. The complements of environmental variables and methodologies used in these studies do differ, limiting extensive comparison between these analyses.

The determinants of vascular plant species are shown to be region specific (Figures **??**, **??**, **??**). The importance of MAP and roughness in rainfall seasonality (PCV) in predicting richness in the SWAFR (Figure **??**I, **??**J), aligns with the steep climatic gradients observed there (Cook et al., 2015). The soil variables that determine plant species richness in the model for the SWAFR (Figures **??**K, **??**L) differ to those that determine richness in the GCFR (Figures **??**G, **??**H), further highlighting the edaphic differences between these two regions. Although both are nutrient leached systems, the SWAFR is flat, with soil-chronosequences (Laliberte et al., 2014; Cook et al., 2015), while the GCFR is mountainous (Cowling et al., 1996; Cramer et al., 2014; Verboom et al., 2017). The importance of roughness in soil density, and absolute texture, in the SWAFR (Figures **??**K, **??**L) highlights the changes in soil that are associable with age of the substrate (e.g. particle size) as being biologically relevant to species richness. The positive effect of soil clay content on species richness in the SWAFR aligns with the findings of Laliberte et al. (2014) that richness in the SWAFR increases with soil age.

NDVI is more heterogeneous across the GCFR than the SWAFR (Figures **??**A). The fact that thermal variables tend to be more rough in the GCFR (Figure **??**A) is likely due to possible covariance of the MODIS/Terra products with topography, as MODIS data used here describes land surface temperature. As the GCFR is topographically rugged, the roughness of NDVI may arise from this. Despite this, NDVI is an integrating variable, which captures information about productivity, light availability, and soil nutrients (Power et al., 2017). The fact that absolute NDVI contributes to predicting species richness in the GCFR, especially at finer spatial scales (Figure **??**E) demonstrates the role of ecological productivity in facilitating the coexistence diverse species assemblages. Environmental heterogeneity, then, is integral to explaining patterns of species richness, but must be considered along with resource- and energy-availability axes. In so much as a diverse environmental space supports more species, the materials and productivity required for biota to thrive are also needed to support species (**???**; Gaston, 2000; Bøhn & Amundsen, 2004; Kreft & Jetz, 2007). As such, my findings, along with those of previous studies (Rensburg et al., 2002; Thuiller et al., 2006; Kreft & Jetz, 2007; Cramer & Verboom, 2016), suggest that there is ecological and evolutionary consequence to resource availability *and* environmental heterogeneity, in that they tend to be positively associated with species richness.

The combined BRT-model of species richness for both regions reveals soil clay content as an important predictor, at coarse spatial scales, despite this variable not being particularly important within each region separately (Figure **??**). Though this model does not strictly consider the regions as separate, this finding may indicate that the relationship between clay content and species richness differs between the regions. So far as clay content can be used to predict species richness, it matters more to those predictions when applied to large sections (i.e. coarse scales) of each regions.

Kreft & Jetz (2007) modelled global terrestrial vascular plant species richness, which focussed on primarily absolute environmental values, underestimated the richness of the Cape flora. Though Kreft & Jetz (2007) did include topographic heterogeneity in their predictor set, topography is often a proxy for more biologically meaningful variables (Cramer & Verboom, 2016). This explains why the inclusion of these variables (e.g. roughness in mean annual precipitation) yields more accurate predictions of species richness. Indeed, Thuiller et al. (2006) also included topographic heterogeneity.@Cramer2016 described 68% of species richness at the QDS scale across South Africa. Regarding the GCFR, depending on whether one consults pseudo-R^2 (Table 3), the ratio of mean predicted to observed richness per grid-cell (Table 5), or the distributions of predicted vs. observed richness values per grid-cell (Figure **??**), I have achieved a similarly suitable level of predictive accuracy. There is, though, still unexplained species richness in light of my models. As Cramer & Verboom (2016), Rensburg et al. (2002), Thuiller et al. (2006), and Mouchet et al. (2015) have done, these macro-ecological models are a-historical. Evolutionary considerations of species richness in geographic space are worthwhile, especially in regions with environments stable over evolutionary time.

The findings here are correlative. There are, however, many proposed mechanisms to explain the correlative signals demonstrated here. My findings support the hypothesis that Mediterranean systems' plant species richness is a function of spatial variability in environmental conditions. This can stimulate diversification, and maintain that diversity by providing a range of habitats for species co-existence. Oligtrophic soils can stimulate an increase in functional diversity, through the evolution of diverse nutrient acquisition strategies (Lambers et al., 2010; Verboom et al., 2017)—e.g. sclerophylly (Cramer et al., 2014; Cook et al., 2015). An aspect of the environment I have neglected to consider is fire, shown to also contribute to predictions here in the GCFR (Cramer & Verboom, 2016). Cardillo (2012) have shown the structuring forces behind species co-occurrence patterns, and thus likely species richness,differ between species-pairs with different post-fire responses and those with similar post-fire responses.

Though the GCFR was correctly predicted to have, on average, more species per grid-cell at HDS and 3QDS

460 scales than the SWAFR, this was not the case for QDS grid-cells (Table 5). This demonstrates that the GCFR is

461 indeed overall more rich in plant species than the SWAFR, but a given HDS in the SWAFR contains fewer

462 species than a given GCFR HDS. Thus, the greater richness in the GCFR is a product of greater turnover in

463 species at spatial scales no more coarse than the HDS. Species turnover is an interesting aspect to species

464 richness studies, as it species turnover is implicit to species-area and co-existence-area relationships (Hart et

465 al., 2017). One could expect patterns of endemism and species turnover to concur with patterns in

466 environmental heterogeneity to some degree.

467 Following from the understanding that functionally diverse assemblages, which are more likely to be more

468 species rich, are likely to arise and/or occur in areas with diverse ecological pressures (Molina-Venegas et al.,

469 2015), one would expect, then, heterogeneous habitats such as those in Mediterranean-type biodiversity

470 hotspots to exhibit high levels functional beta diversity along steep environmental gradients (Molina-Venegas

471 et al., 2015). If the niches concerning these functions are phylogenetically conserved among those biota, then

472 one would also expect high levels of species and phylogenetic beta diversity along these gradients

473 (Molina-Venegas et al., 2015). This concurs with the notion put forward by Power et al. (2017), wherein

474 megadiverse systems such as these represent the results of "phylogenetic niche conservatism on a

475 heterogeneous landscape". Thus, species and phylogenetic turnover should covary with environmental

476 heterogeneity in some way. Indeed, endemism, at certain scales, could also follow this pattern. Thuiller et al.

477 (2006) demonstrated that there is phylogenetic and biome related determinants of species richness. This makes

478 sense, in light of the difficulty of crossing biome boundaries in Mediterranean systems (Power et al., 2017).

479 NDVI and light availability, and the heterogeneity therein, are associated with high levels of floristic turnover

480 (Power et al., 2017). This may be indicative of ecological specialisation precluding species from crossing these

481 boundaries, thus increasing the level of endemism within a region, while also increasing the level of turnover,

482 and thus likely species richness, along environmental gradients. Although, this may be debated. Beard et al.

483 (2000) state that the high levels of endemism in SWAFR are function of habitat specialisation to soil mosaics.

484 Cf. Laliberte et al. (2014), who say that this endemism is likely due to environmental filtering along these soil

485 turnover sequences, as opposed to the juxtaposition of specialised species along soil gradients.

486 I have demonstrated support for the idea that environmental heterogeneity is positively associated with species

487 richness, particularly Mediterranean systems. In the SWAFR and the GCFR, high levels of endemism and

488 biodiversity are also likely the results of long-term landscape and climatic stability (Hopper, 1979). Thus, the

489 roles of environmental variability through space, and stability through time, are the two main ways in which the

490 environment relates to biodiversity in these regions.

4.1 Future studies (a.k.a. "to do after first review")

- 3QDS scale BRTs
- $S_{\mathrm{HDS}} \sim \overline{S}_{\mathrm{QDS}} + \overline{\delta_{ij}}_{??}$ (= "$\gamma = \alpha + \beta$"-analysis) (see `explore-turnover-metrics.pdf` note, where $\overline{\delta_{ij}}(\mathbf{N})_{??} = \overline{\alpha_i}(\mathbf{N}) \times \overline{\beta_{ij}}(\mathbf{N}) = \overline{S}_{\mathrm{QDS}} \times \overline{J}_{\mathrm{QDS}}$)

Table captions

Captions are also repeated alongside their respective tables for readability.

Table 1: Georeferenced vascular plant species occurence and environmental data sources used in this study. Data were acquired for the Cape and SWA regions, with the temporal extent of data products used described where applicable. Abbreviations are as follows: MAP, mean annual precipitation; PDQ, precipitation in the driest quarter; CEC, cation exchange capacity.

Table 2: Average percentile-ranks for BRT-model performance measures (nt, R^2_{pseudo} (Equation (4)), $R^2_{\mathrm{E-O}}$) of 1000 replicate BRT-models relative to 999 BRT-models fit to permuted datasets. Ranks approaching one indicate that a set of replicate BRT-models had greater values than the permuted models.

Table 3: Estimated differences between replicate Cape and SWA BRT-models' performance measures (nt, R^2_{pseudo} (Equation (4)), $R^2_{\mathrm{E-O}}$) following t-tests. Positive values indicate that the Cape models had greater values. In all cases, the Cape and SWA had highly significantly different values for these quality measures ($P < 0.0001$).

Figure captions

Captions are also repeated alongside their respective figures for readability.

Figure 1: Comparisons of different types of environmental heterogeneity between the the Greater Cape Floristic Region (Cape) and the Southwest Australia Floristic Region (SWA). We present (a) distributions of roughness values (Equation (1)) for example variables from each broad category of the environment concerned. (b) The common language effect size ($CLES$; see text) of Cape versus SWA roughness values is shown for all variables, grouped by broad categories of the environment, describing differences in the distributions of Cape

20

515 and SWA roughness values. We used Mann-Whitney U-tests to assess differences in these distributions.

516 Non-significant differences ($P_U > 0.05$) are denoted as such ("NS"). Note, U-tests were performed using only

517 a random set of 5000 cells at the 0.05-degree-scale, as the U-test as implemented in R cannot handle more than

518 that many values to compare.

519 Figure 2: Species turnover, described in two forms ((a) mean Jaccard distance between QDS in each HDS

520 ($\overline{J}_{\text{QDS}}$), (b) additively defined turnover (T_{HDS}, Equation (2)) as a proportion of HDS richness (S_{HDS})),

521 compared between the Cape and SWA. Mann-Whitney U-tests between the Cape and SWA distributions of

522 $\overline{J}_{\text{QDS}}$ and T_{HDS} yielded significant differences.

523 Figure 3: Relative influence of environmental variables (including heterogeneity variables—prefixed with "R")

524 in boosted regression tree (BRT) model predictions in the Greater Cape Floristic Region (Cape, a–c) and the

525 Southwest Australia Floristic Region (SWA, b–d) of vascular plant species richness at the (b,e) QDS-scale

526 ($= \overline{S}_{\text{QDS}}$), (a,d) HDS-scale ($= S_{\text{HDS}}$) and (c,f) turnover ($= \overline{J}_{\text{QDS}}$). All BRT-models were permitted to fit

527 three-way interactions between environmental variables. Points denote the mean contribution of an

528 environmental variable to model-predictions across the 1000 replicate BRT-models for that region/scope.

529 Horizontal ticks denote the mean for the 999 permuted BRT-models. Standard deviations above and below

530 these means are shown with vertical lines. Note, in the case of the replicate, standard deviations are so small

531 such that the vertical lines are obscured by the points. Colours represent the general category of the

532 environment to which a variable belongs (keyed), as in Figure 1b. Left-most piecharts inset in each panel

533 display the same information. Right-most piecharts group contributions according to whether a variable was

534 absolute or roughness-transformed (keyed). F-statistics inset are for one-way ANOVAs of differences in

535 variables' relative influences—for both the replicate ($F_{\text{rep.}}$) and permuted ($F_{\text{prm.}}$) BRT-models.

536 Figure 4: Distributions of three measures of boosted regression tree (BRT) model performance: (a) the number

537 of trees in the model nt, (b) R^2_{pseudo} (Equation (4)), (c) $R^2_{\text{E-O}}$ (see text). These measures are presented for the

538 six sets of permuted (pale bars) and six sets of replicate BRT-models (dark bars) as in Figure 3, coloured

539 according to the region of interest as in Figures 1a and 2. In all cases, replicate BRT-models almost entirely

540 out-rank the permuted models in terms of performance (Table 2) and the Greater Cape Floristic Region (Cape)

541 and Southwest Australia Floristic Region (SWA) models had significantly different values for each metric

542 (Table 3). Note, the actual differences between Cape and the SWA models' values is not realistically significant

543 in some cases (e.g. the difference in nt between the Cape and SWA QDS richness models is statistically

544 significant, but are observedly so similar as not to affect interpretation).

21

Figure 5: Differences in the rankings of environmental variables' (including heterogeneity variables) relative influences on boosted regression tree (BRT) model predictions of vascular plant species richness and turnover in (a) the Greater Cape Floristic Region (Cape) and (b) Southwest Australia Floristic Region (SWA) (as in Figure 3). Each point represents an environmental variable's rank in BRT-model importance, decreasing in importance from left to right. Rankings used here are the same as that of the average relative influence for variables across replicate BRT-models, presented in Figure 3. Coloured lines connect points representing the same environmental variable. Points' outlines are coloured according to the general category of the environment (keyed) to which a variable belongs, as in Figuress 1b and 3, while points' centres are coloured according to whether a variable was roughness-transformed or not. The comparisons of variables' rankings of interest are between QDS- and HDS-scale richness (= $\overline{S}_{\mathrm{QDS}}$ and S_{HDS} respectively; rows nos. 1 and 2) and between HDS-scale richness and turnover (= $\overline{J}_{\mathrm{QDS}}$) (rows nos. 2 and 3). Statistics (Δ- and P-values) inset at the top and bottom of each panel refer to these comparisons respectively. Δ-values represent the average absolute difference in ranks across variables between two models' rankings. The associate P-value results from ranking the observed Δ-values against 999 Δ-values based on random permutations of variables' rankings (SI1), such that more significant P-values denote rankings more similar than would be expected by chance.

Figure 6: Marginal effects of environmental conditions and heterogeneity on vascular plant species richness at the QDS-scale (= $\overline{S}_{\mathrm{QDS}}$; a,d), HDS-scale (= S_{HDS}; b,e) and turnover (= $\overline{J}_{\mathrm{QDS}}$; c,f) in response variables in the Greater Cape Floristic Region (Cape; a–c) and Southwest Australia Floristic Region (SWA; d–f) following boosted regression tree (BRT) modelling. Marginal effect functions presented are derived from a representative BRT-model from the set of replicate BRT-models (for each of the six modelling cases) (see SI regarding how representative BRT-models were selected). Marginal effects represent the effect of a predictor variable when all other predictors are set at their means. Marginal effect functions are shown for environmental variables that contributed $\geq 10\%$ to a model's predictions. Functions are coloured as keyed, with solid lines representing absolute environmental variables and dotted representing heterogeneity variables ("rough"). Environmental variables were all rescaled here such as to be centred on zero (i.e. Z-transformed), facilitating comparison of functions' forms.

References

Baudena, M., Sánchez, A., Georg, C.-P., Ruiz-Benito, P., Rodríguez, M.Á., Zavala, M.A., & Rietkerk, M. (2015) Revealing patterns of local species richness along environmental gradients with a novel network tool. *Scientific Reports*, **5**, 11561.

574   Beard, J.S., Chapman, A.R., & Gioia, P. (2000) Species richness and endemism in the Western Australian flora. *Journal of*
575   *Biogeography*, **27**, 1257–1268.

576   Bradshaw, P.L. & Cowling, R.M. (2014) Landscapes, rock types, and climate of the Greater Cape Floristic Region. *Fynbos: Ecology,*
577   *evolution and conservation of a megadiverse region* (ed. by N. Allsopp, J.F. Colville, and G.A. Verboom), pp. 26–46.
578   Oxford University Press, Oxford.

579   Bøhn, T. & Amundsen, P.-A. (2004) Ecological Interactions and Evolution: Forgotten Parts of Biodiversity? *BioScience*, **54**, 804.

580   Cardillo, M. (2012) The phylogenetic signal of species co-occurrence in high-diversity shrublands: different patterns for fire-killed and
581   fire-resistant species. *BMC Ecology*, **12**, 21.

582   Cook, L.G., Hardy, N.B., & Crisp, M.D. (2015) Three explanations for biodiversity hotspots: small range size, geographical overlap
583   and time for species accumulation. An Australian case study. *New Phytologist*, **207**, 390–400.

584   Cowling, R.M., Rundel, P.W., Lamont, B.B., Arroyo, M.K., & Arianoutsou, M. (1996) Plant diversity in mediterranean-climate regions.
585   *Trends in Ecology and Evolution*, **11**, 362–366.

586   Cramer, M.D. & Verboom, G.A. (2016) Measures of biologically relevant environmental heterogeneity improve prediction of regional
587   plant species richness. *Journal of Biogeography*, 1–13.

588   Cramer, M.D., West, A.G., Power, S.C., Skelton, R., & Stock, W.D. (2014) Plant ecophysiological diversity. *Fynbos: Ecology,*
589   *evolution and conservation of a megadiverse region* pp. 248–272. Oxford University Press, Oxford.

590   Deblauwe, V., Droissart, V., Bose, R., Sonké, B., Blach-Overgaard, A., Svenning, J.C., Wieringa, J.J., Ramesh, B.R., Stévart, T., &
591   Couvreur, T.L.P. (2016) Remotely sensed temperature and precipitation data improve species distribution modelling in the
592   tropics. *Global Ecology and Biogeography*, **25**, 443–454.

593   Elith, J., Leathwick, J.R., & Hastie, T. (2008) A working guide to boosted regression trees. *Journal of Animal Ecology*, **77**, 802–813.

594   Farr, T., Rosen, P., Caro, E., Crippen, R., Duren, R., Hensley, S., Kobrick, M., Paller, M., Rodriguez, E., Roth, L., Seal, D., Shaffer, S.,
595   Shimada, J., Umland, J., Werner, M., Oskin, M., Burbank, D., & Alsdorf, D. (2007) The shuttle radar topography mission.
596   *Reviews of Geophysics*, **45**, 1–33.

597   Funk, C.C., Peterson, P.J., Landsfeld, M., Pedreros, D.H., Verdin, J., Shukla, S., Husak, G., Rowland, J.D., Harrison, L., Hoell, A., &
598   Michaelsen, J. (2015) The climate hazards infrared precipitation with stations—a new environmental record for monitoring
599   extremes. *Scientific Data*, **2**, 150066.

600   Gaston, K.J. (2000) Global patterns in biodiversity. *Nature*, **405**, 220–227.

601   GBIF (24 July 2017) GBIF Occurrence Download..

602   GBIF (24 July 2017) GBIF Occurrence Download..

603   Gioia, P. & Hopper, S.D. (2017) A new phytogeographic map for the Southwest Australian Floristic Region after an exceptional decade

604   of collection and discovery. *Botanical Journal of the Linnean Society*, **184**, 1–15.

605   Hart, S.P., Usinowicz, J., & Levine, J.M. (2017) The spatial scales of species coexistence. *Nature Ecology & Evolution*, **1**, 1066–1073.

606   Hengl, T., Mendes de Jesus, J., Heuvelink, G.B.M., Ruiperez Gonzalez, M., Kilibarda, M., Blagoti?, A., Shangguan, W., Wright, M.N.,
607   Geng, X., Bauer-Marschallinger, B., Guevara, M.A., Vargas, R., MacMillan, R.A., Batjes, N.H., Leenaars, J.G.B., Ribeiro, E.,
608   Wheeler, I., Mantel, S., & Kempen, B. (2017) SoilGrids250m: Global gridded soil information based on machine learning.
609   *PLoS ONE*, **12**, e0169748.

610   Hopper, S.D. (1979) Biogeographical Aspects of Speciation in the Southwest Australian Flora. *Annual Review of Ecology and*
611   *Systematics*, **10**, 399–422.

612   Hopper, S.D. & Gioia, P. (2004) The Southwest Australian Floristic Region: Evolution and Conservation of a Global Hot Spot of
613   Biodiversity. *Annual Review of Ecology, Evolution, and Systematics*, **35**, 623–650.

614   Kreft, H. & Jetz, W. (2007) Global patterns and determinants of vascular plant diversity. *Proceedings of the National Academy of*
615   *Sciences*, **104**, 5925–5930.

616   Laliberte, E., Zemunik, G., & Turner, B.L. (2014) Environmental filtering explains variation in plant diversity along resource gradients.
617   *Science*, **345**, 1602–1605.

618   Lambers, H., Brundrett, M.C., Raven, J.A., & Hopper, S.D. (2010) Plant mineral nutrition in ancient landscapes: high plant species
619   diversity on infertile soils is linked to functional diversity for nutritional strategies. *Plant and Soil*, **334**, 11–31.

620   Larsen, R., Holmern, T., Prager, S.D., Maliti, H., & Røskaft, E. (2009) Using the extended quarter degree grid cell system to unify
621   mapping and sharing of biodiversity data. *African Journal of Ecology*, **47**, 382–392.

622   Levin, L.A., Sibuet, M., Gooday, A.J., Smith, C.R., & Vanreusel, A. (2010) The roles of habitat heterogeneity in generating and
623   maintaining biodiversity on continental margins: an introduction. *Marine Ecology*, **31**, 1–5.

624   Lobo, J.M., Jay-robert, P., Lumaret, J.-p., Lobo, J.M., Jay-robert, P., & Lumaret, J.-p. (2004) Modelling the Species Richness
625   Distribution for French Aphodiidae (Coleoptera, Scarabaeoidea). *Ecography*, **27**, 145–156.

626   Mateo, R.G., Mokany, K., & Guisan, A. (2017) Biodiversity Models: What If Unsaturation Is the Rule? *Trends in Ecology &*
627   *Evolution*, **32**, 556–566.

628   Molina-Venegas, R., Aparicio, A., Slingsby, J.A., Lavergne, S., & Arroyo, J. (2015) Investigating the evolutionary assembly of a
629   Mediterranean biodiversity hotspot: Deep phylogenetic signal in the distribution of eudicots across elevational belts. *Journal*
630   *of Biogeography*, **42**, 507–518.

631   Mouchet, M., Levers, C., Zupan, L., Kuemmerle, T., Plutzar, C., Erb, K., Lavorel, S., Thuiller, W., & Haberl, H. (2015) Testing the
632   effectiveness of environmental variables to explain European terrestrial vertebrate species richness across biogeographical
633   scales. *PLoS ONE*, **10**, 1–16.

634   Mucina, L. & Rutherford, M.C. (2006) *The vegetation of South Africa, Lesotho and Swaziland.* South African National Biodiversity
635   Institute,

636   NIMA (2000) Amendment 1. 3 January 2000. Department of Defense World Geodetic System 1984. Its Definition and Relationships
637   with Local Geodetic Systems. 1–3.

638   Olson, D.M., Dinerstein, E., Wikramanayake, E.D., Burgess, N.D., Powell, G.V.N., Underwood, E.C., D'amico, J.A., Itoua, I., Strand,
639   H.E., Morrison, J.C., & Others (2001) Terrestrial Ecoregions of the World: A New Map of Life on Earth: A new global map of
640   terrestrial ecoregions provides an innovative tool for conserving biodiversity. *BioScience*, **51**, 933–938.

641   Power, S.C., Verboom, G.A., Bond, W.J., & Cramer, M.D. (2017) Environmental correlates of biome-level floristic turnover in South
642   Africa. *Journal of Biogeography*, **44**, 1745–1757.

643   R Core Team (2018) *R: A Language and Environment for Statistical Computing. Version 3.5.0.* R Foundation for Statistical
644   Computing, Vienna, Austria.

645   Rensburg, B.J. van, Chown, S.L., & Gaston, K.J. (2002) Species Richness, Environmental Correlates, and Spatial Scale: A Test Using
646   South African Birds. *The American Naturalist*, **159**, 566–577.

647   Ricklefs, R.E. (1987) Community diversity: relative roles of local and regional processes. *Science, New Series*, **235**, 167–171.

648   Thuiller, W., Midgley, G.F., Rouget, M., Cowling, R.M., F. Midgley, G., Rougeti, M., & M. Cowling, R. (2006) Predicting patterns of
649   plant species richness in megadiverse South Africa. *Ecography*, **29**, 733–744.

650   Verboom, G.A., Stock, W.D., & Cramer, M.D. (2017) Specialization to extremely low-nutrient soils limits the nutritional adaptability
651   of plant lineages. *The American Naturalist*, **In press**,.

652   Wardell-Johnson, G. & Horwitz, P. (1996) Conserving biodiversity and the recognition of heterogeneity in ancient landscapes: a case
653   study from south-western Australia. *Forest Ecology and Management*, **85**, 219–238.

Biosketches

Ruan van Mazijk is a Masters student interested in phylogenetic systematics, macro-ecology, comparative work and plant functional ecology.

Michael D. Cramer

G. Anthony Verboom

Author contributions

MDC and GAV conceived the study question, which RVM investigated under their supervision for his BSc Hons project. The analyses and programming work were largely devised by RVM, with input from the other authors, and was carried out by RVM. RVM wrote the first draft of the manuscript and all authors contributed equally thereafter.

Tables

Table 1: Georeferenced vascular plant species occurence and environmental data sources used in this study. Data were acquired for the Cape and SWA regions, with the temporal extent of data products used described where applicable. Abbreviations are as follows: MAP, mean annual precipitation; PDQ, precipitation in the driest quarter; CEC, cation exchange capacity.

Variable	Source	Temporal extent	Citation
Plant species occurrences	GBIF	TODO	**??, ??**
Elevation	SRTM v2.0		**??**
NDVI	MODIS (MOD13C2)	Feb. 2000 to Apr. 2017	**??**
Climatic variables			
Surface temperature	MODIS (MOD11C3)	Feb. 2000 to Apr. 2017	**??**
MAP	CHIRPS v2.0	Jan. 1981 to Feb. 2017	**??**
PDQ	CHIRPS v2.0	Jan. 1981 to Feb. 2017	**??**
Soil variables			
CEC	SoilGrids250m (CECSOL M 250m)		**??**
Clay	SoilGrids250m (CLYPPT M 250m)		
Soil C	SoilGrids250m (OCDENS M 250m)		
pH	SoilGrids250m (PHIKCL M 250m)		

Table 2: Average percentile-ranks for BRT-model performance measures (nt, R^2_{pseudo} (Equation (4)), $R^2_{\text{E}-\text{O}}$) of 1000 replicate BRT-models relative to 999 BRT-models fit to permuted datasets. Ranks approaching one indicate that a set of replicate BRT-models had greater values than the permuted models.

Model	nt	R^2_{pseudo}	R^2_{E-O}
QDS-richness			
GCFR	1.000	1.000	1.000
SWAFR	1.000	1.000	1.000
HDS-richness			
GCFR	0.987	1.000	0.988
SWAFR	1.000	1.000	1.000
HDS-turnover			
GCFR	0.977	0.992	0.979
SWAFR	0.997	1.000	1.000

Table 3: Estimated differences between replicate Cape and SWA BRT-models' performance measures (nt, R^2_{pseudo} (Equation (4)), $R^2_{\text{E}-\text{O}}$) following t-tests. Positive values indicate that the Cape models had greater values. In all cases, the Cape and SWA had highly significantly different values for these quality measures ($P < 0.0001$).

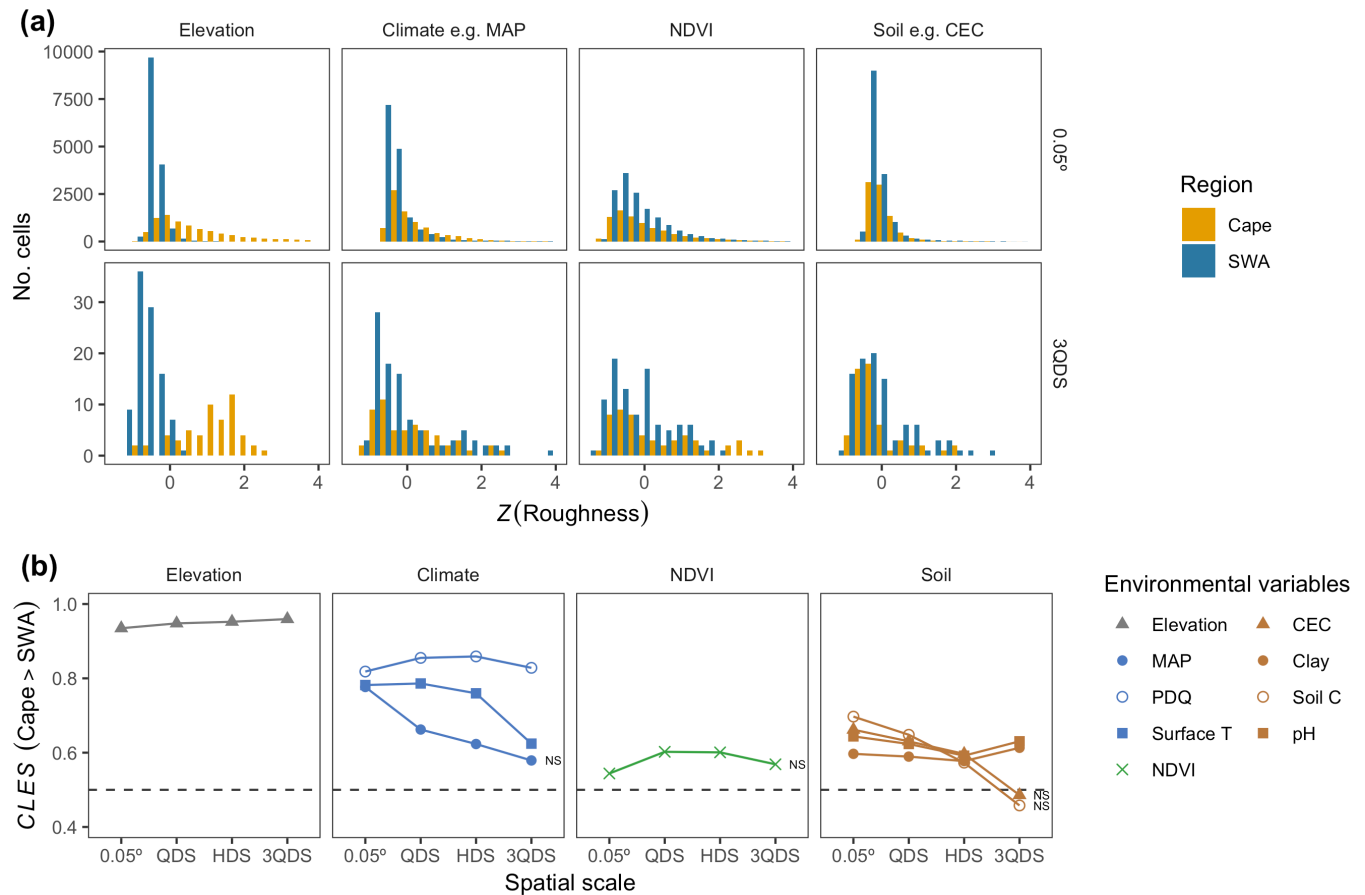| Model	nt	R^2_{pseudo}	$R^2_{\text{E}-\text{O}}$
QDS-richness	542.938	0.063	-0.005
HDS-richness	-808.994	-0.064	-0.233
HDS-turnover	-997.045	-0.052	-0.296

Figures

Figure 1: Comparisons of different types of environmental heterogeneity between the the Greater Cape Floristic Region (Cape) and the Southwest Australia Floristic Region (SWA). We present (a) distributions of roughness values (Equation (1)) for example variables from each broad category of the environment concerned. (b) The common language effect size ($CLES$; see text) of Cape versus SWA roughness values is shown for all variables, grouped by broad categories of the environment, describing differences in the distributions of Cape and SWA roughness values. We used Mann-Whitney U-tests to assess differences in these distributions. Non-significant differences ($P_U > 0.05$) are denoted as such ("NS"). Note, U-tests were performed using only a random set of 5000 cells at the 0.05-degree-scale, as the U-test as implemented in R cannot handle more than that many values to compare.
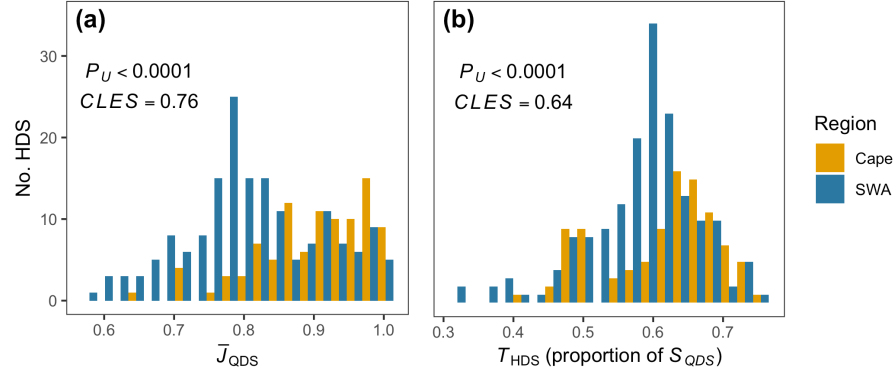
Figure 2: Species turnover, described in two forms ((a) mean Jaccard distance between QDS in each HDS ($\overline{J}_{\mathrm{QDS}}$), (b) additively defined turnover (T_{HDS}, Equation (2)) as a proportion of HDS richness (S_{HDS})), compared between the Cape and SWA. Mann-Whitney U-tests between the Cape and SWA distributions of $\overline{J}_{\mathrm{QDS}}$ and T_{HDS} yielded significant differences.
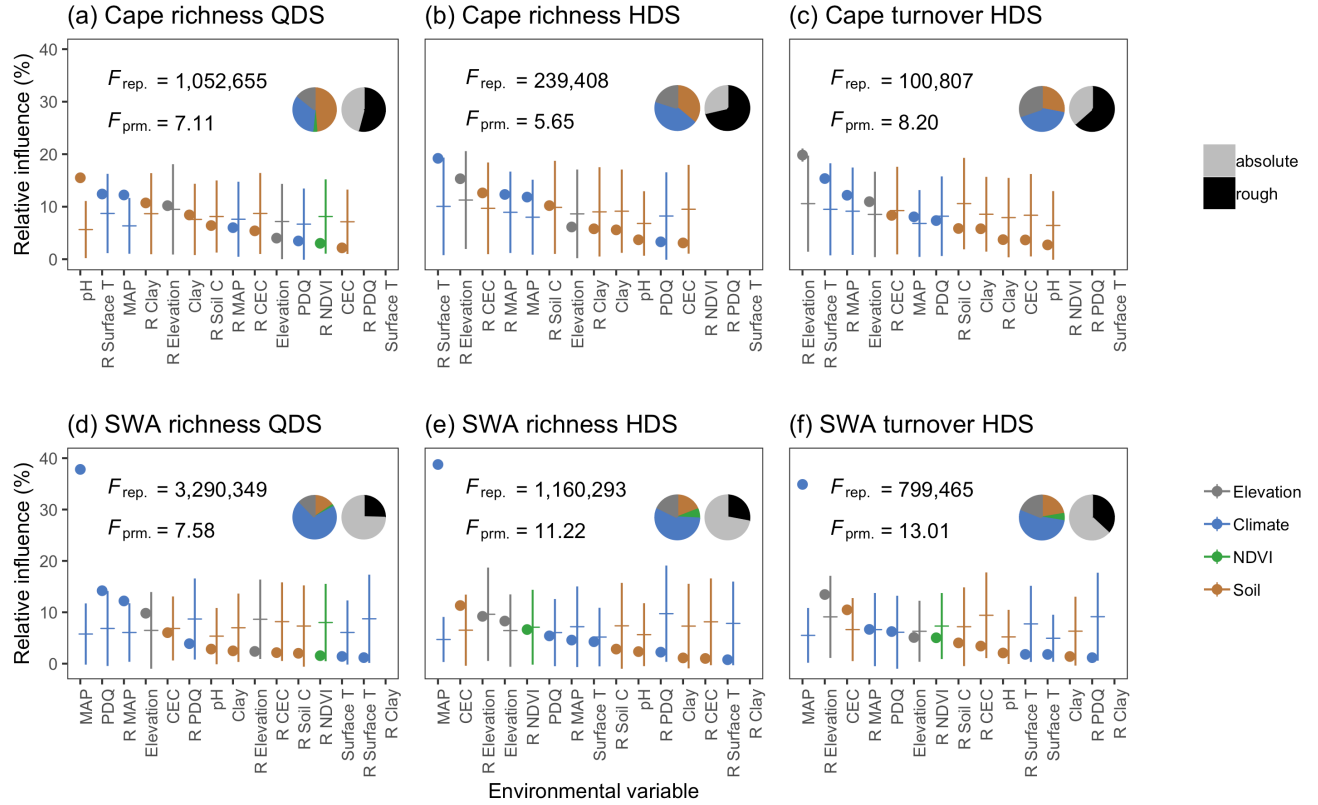
Figure 3: Relative influence of environmental variables (including heterogeneity variables—prefixed with "R") in boosted regression tree (BRT) model predictions in the Greater Cape Floristic Region (Cape, a–c) and the Southwest Australia Floristic Region (SWA, b–d) of vascular plant species richness at the (b,e) QDS-scale ($= \overline{S}_{\mathrm{QDS}}$), (a,d) HDS-scale ($= S_{\mathrm{HDS}}$) and (c,f) turnover ($= \overline{J}_{\mathrm{QDS}}$). All BRT-models were permitted to fit three-way interactions between environmental variables. Points denote the mean contribution of an environmental variable to model-predictions across the 1000 replicate BRT-models for that region/scope. Horizontal ticks denote the mean for the 999 permuted BRT-models. Standard deviations above and below these means are shown with vertical lines. Note, in the case of the replicate, standard deviations are so small such that the vertical lines are obscured by the points. Colours represent the general category of the environment to which a variable belongs (keyed), as in Figure 1b. Left-most piecharts inset in each panel display the same information. Right-most piecharts group contributions according to whether a variable was absolute or roughness-transformed (keyed). F-statistics inset are for one-way ANOVAs of differences in variables' relative influences—for both the replicate ($F_{\mathrm{rep.}}$) and permuted ($F_{\mathrm{prm.}}$) BRT-models.
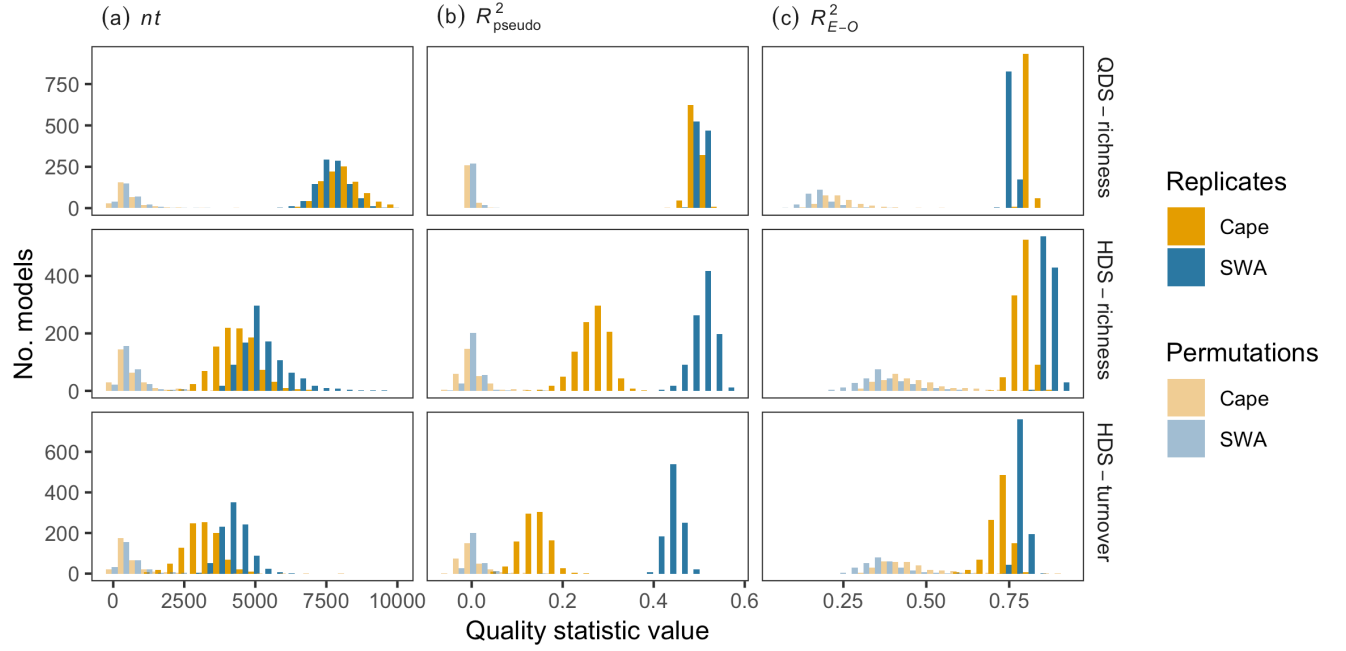
31

Figure 4: Distributions of three measures of boosted regression tree (BRT) model performance: (a) the number of trees in the model nt, (b) R^2_{pseudo} (Equation (4)), (c) $R^2_{\text{E}-\text{O}}$ (see text). These measures are presented for the six sets of permuted (pale bars) and six sets of replicate BRT-models (dark bars) as in Figure 3, coloured according to the region of interest as in Figures 1a and 2. In all cases, replicate BRT-models almost entirely out-rank the permuted models in terms of performance (Table 2) and the Greater Cape Floristic Region (Cape) and Southwest Australia Floristic Region (SWA) models had significantly different values for each metric (Table 3). Note, the actual differences between Cape and the SWA models' values is not realistically significant in some cases (e.g. the difference in nt between the Cape and SWA QDS richness models is statistically significant, but are observedly so similar as not to affect interpretation).
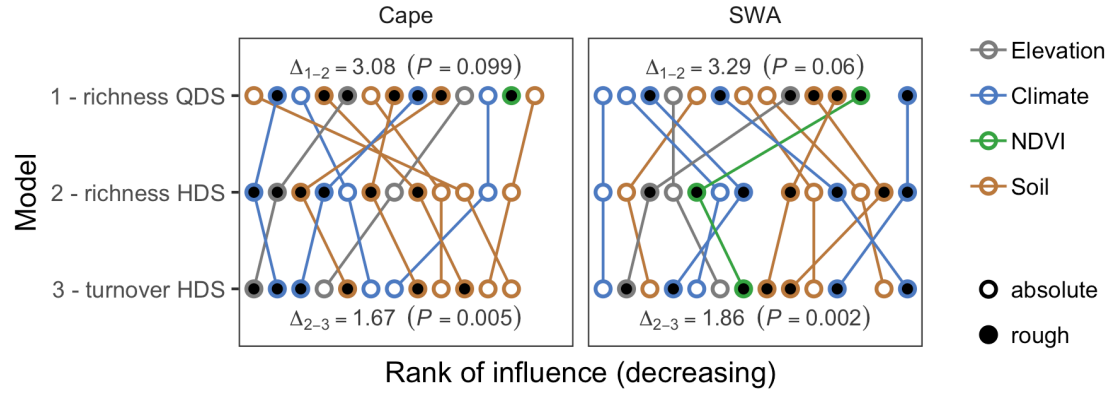
Figure 5: Differences in the rankings of environmental variables' (including heterogeneity variables) relative influences on boosted regression tree (BRT) model predictions of vascular plant species richness and turnover in (a) the Greater Cape Floristic Region (Cape) and (b) Southwest Australia Floristic Region (SWA) (as in Figure 3). Each point represents an environmental variable's rank in BRT-model importance, decreasing in importance from left to right. Rankings used here are the same as that of the average relative influence for variables across replicate BRT-models, presented in Figure 3. Coloured lines connect points representing the same environmental variable. Points' outlines are coloured according to the general category of the environment (keyed) to which a variable belongs, as in Figuress 1b and 3, while points' centres are coloured according to whether a variable was roughness-transformed or not. The comparisons of variables' rankings of interest are between QDS- and HDS-scale richness (= $\overline{S}_{QDS}$ and S_{HDS} respectively; rows nos. 1 and 2) and between HDS-scale richness and turnover (= $\overline{J}_{QDS}$) (rows nos. 2 and 3). Statistics (Δ- and P-values) inset at the top and bottom of each panel refer to these comparisons respectively. Δ-values represent the average absolute difference in ranks across variables between two models' rankings. The associate P-value results from ranking the observed Δ-values against 999 Δ-values based on random permutations of variables' rankings (SI1), such that more significant P-values denote rankings more similar than would be expected by chance.
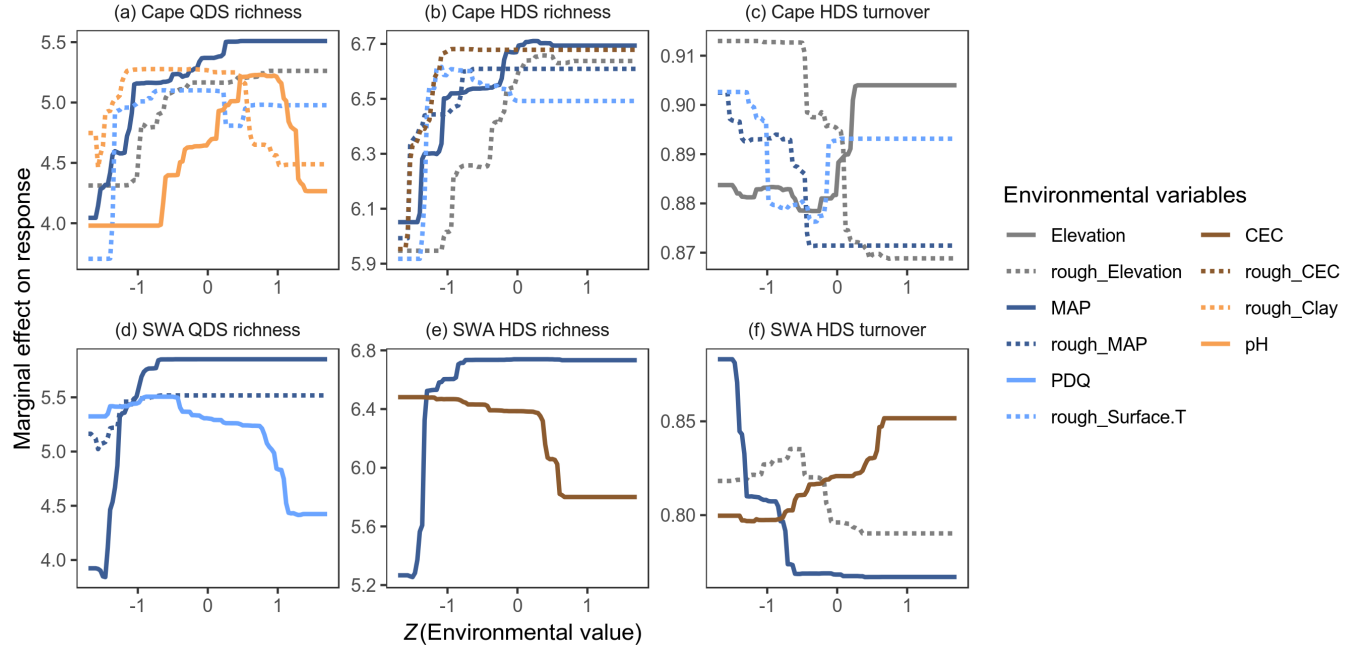
Figure 6: Marginal effects of environmental conditions and heterogeneity on vascular plant species richness at the QDS-scale (= $\overline{S}_{\text{QDS}}$; a,d), HDS-scale (= S_{HDS}; b,e) and turnover (= $\overline{J}_{\text{QDS}}$; c,f) in response variables in the Greater Cape Floristic Region (Cape; a–c) and Southwest Australia Floristic Region (SWA; d–f) following boosted regression tree (BRT) modelling. Marginal effect functions presented are derived from a representative BRT-model from the set of replicate BRT-models (for each of the six modelling cases) (see SI regarding how representative BRT-models were selected). Marginal effects represent the effect of a predictor variable when all other predictors are set at their means. Marginal effect functions are shown for environmental variables that contributed $\geq 10\%$ to a model's predictions. Functions are coloured as keyed, with solid lines representing absolute environmental variables and dotted representing heterogeneity variables ("rough"). Environmental variables were all rescaled here such as to be centred on zero (i.e. Z-transformed), facilitating comparison of functions' forms.